Asymptotic model of the inertial migration of particles in a dilute suspension flow through the entry region of a channel

Andrei A. Osiptsov[1,a] and Evgeny S. Asmolov[1,2]
[1]*Department of Geomechanics, Schlumberger Moscow Research, Moscow 101000, Russia*
[2]*Central Aero-Hydrodynamics Institute, Zhukovsky, Moscow Region 140180, Russia*

(Received 5 June 2008; accepted 2 November 2008; published online 3 December 2008)

The inertial migration of particles in a dilute suspension flow through the entry region of a plane channel (or a circular pipe) is considered. Within the two-fluid approach, an asymptotic one-way coupling model of the dilute suspension flow in the entry region of a channel is constructed. The carrier phase is a viscous incompressible Newtonian fluid, and the dispersed phase consists of identical noncolloidal rigid spheres. In the interphase momentum exchange, we take into account the drag force, the virtual mass force, the Archimedes force, and the inertial lift force with a correction factor due to the wall effect and an arbitrary particle slip velocity. The channel Reynolds number is high and the particle-to-fluid density ratio is of order unity or significantly larger unity. The solution is constructed using the matched asymptotic expansion method. The problem of finding the far-downstream cross-channel profile of particle number concentration is reduced to solving the equations of the two-phase boundary layer developing on the channel walls. The full Lagrangian approach is used to study the evolution of the cross-flow particle concentration profile. The inertial migration results in particle accumulation on two symmetric planes (an annulus) distanced from the walls, with a nonuniform concentration profile between the planes (inside the annulus) and particle-free layers near the walls. When the particle-to-fluid density ratio is of order unity, an additional local maximum of the particle concentration on inner planes (an inner annulus) is revealed. The inclusion of the corrected lift force makes it possible to resolve the nonintegrable singularity in the concentration profile on the wall, which persisted in all previously published solutions for the dilute suspension flow in a boundary layer. The numerical results are compared to the tubular pinch effect observed in experiments, and a qualitative analogy is found.
 [DOI: 10.1063/1.3032909]

I. INTRODUCTION

The problem of inertial migration of particles in suspension flows has received considerable attention from the scientific community over the past 50 years because of its importance in a wide range of applications. Examples of particulate flows involving migration phenomena arise in many disciplines, from small-scale biomechanics (transport of corpuscles in blood vessels) toward large-scale environmental fluid mechanics (atmospheric dusty-gas flows), including many mesoscale industrial applications (e.g., transport and migration of proppant particles in oil wells or hydraulic fractures).

Most theoretical papers focus on evaluating the inertial lift force that causes lateral migration of particles in shear flows of a viscous fluid under different conditions (effects of the particle slip, rotation, and oscillation, and effects of the presence of a rigid boundary and gravitational settling).[1] Segre and Silberberg[2] showed that neutrally buoyant particles suspended in a Poiseuille flow at low channel Reynolds numbers through a tube migrate in the cross-flow direction toward a steady position at 0.6 of the tube radius from the axis. Using the method of matched asymptotic expansions, Saffman[3] obtained the lift force on a small sphere moving with a nonzero slip velocity parallel to an unbounded linear shear flow. This result was found in the strong shear limit, when the particle Reynolds numbers based on the slip velocity U_s and the shear rate G, $\mathrm{Re}_s=2\sigma U_s\rho/\mu$ and $\mathrm{Re}_G=4\sigma^2 G\rho/\mu$, are both small and related as $\mathrm{Re}_s/\mathrm{Re}_G^{1/2}\ll 1$. Here, σ is the particle radius, and ρ and μ are fluid density and viscosity. Asymptotic solutions in the inner region on the length scale σ and the outer region on the length scale $L_{\mathrm{Saff}}=(\mu/\rho G)^{1/2}\gg\sigma$ were obtained. It was demonstrated that the lift force is caused by a nonzero transverse component of the outer disturbance flow at the particle center.

Subsequent studies extended this result to take into account the effects of either a nonzero slip parameter $\chi=\mathrm{Re}_s/\mathrm{Re}_G^{1/2}$ or the presence of a rigid impermeable wall. Cox and Hsu[4] calculated the migration velocity of a particle sedimenting in a stagnant fluid bounded by a plane wall. Asmolov[5] and McLaughlin[6] extended Saffman's analysis to the case of an unbounded flow when χ takes finite nonzero values. Additionally, Asmolov[5] and McLaughlin[7] addressed the wall effect and obtained the inertial lift force for the case when a particle moves parallel to a flat rigid wall in a linear shear flow at distances that are large compared to the particle radius. The migration velocity was tabulated[7] as a function of the slip parameter and the distance from the wall scaled by L_{Saff}. The approximate formulas for the dependence of the

[a]Author to whom correspondence should be addressed. Electronic mail: aosiptsov@slb.com.

migration velocity on the slip parameter χ were proposed by Asmolov[8] and Mei.[9]

The inertial migration of a non-neutrally buoyant particle translating parallel to the walls within a channel flow was investigated at finite[10,11] and large[12] channel Reynolds numbers Re. At large Re, the wall effect is important in near-wall layers of the thickness $d\,\mathrm{Re}^{-1/2}$, where the migration velocity is close to that calculated for a linear wall-bounded flow.[5,7] The wall effect can be neglected within the core of the flow, and the disturbance flow can be treated as unbounded. However, the inertial lift in this region differs from the predictions for a linear flow[5,6] because of the effect of curvature of the Poiseuille velocity profile.

A relatively smaller number of papers are devoted to studying the evolution of the particle concentration profile as a result of inertial migration of particles in suspension flows, when both the carrier fluid and the particles are considered within the continuum approach. Continuum modeling of the fluid-particle boundary layer was reviewed by Marble[13] and Osiptsov.[14] A two-continua model of the dusty-gas boundary layer on a flat plate was presented for the case when only the Stokes force is taken into account.[15] It was shown[16] that the cross-flow profile of particle number concentration contains a nonintegrable singularity on the wall, i.e., the number concentration of particles grows infinitely as the wall is approached and the integral of particle concentration over the cross-flow coordinate diverges near the wall. It was demonstrated[16] that in the vicinity of a nonintegrable singularity the mean distance between particles is not large compared to the particle radius. Hence, the medium of particles is not dilute and the interparticle interactions should be taken into account in the vicinity of the singularity. However, in the case when the particle number concentration tends to infinity, but the singularity is integrable, the mean distance between particles remains significantly larger than the particle radius and the basic assumption of the dilute suspension model is valid.[16]

The cross-flow particle migration due to the classical Saffman lift force was studied for dusty-gas flows in a channel using the Lagrangian approach[17] and in a boundary layer using the Eulerian approach.[18] Foster *et al.*[18] also presented a survey of more recent advances in continuum modeling of dilute suspension flows. The correction to the lift due to a nonzero value of the slip parameter was taken into account for boundary-layer flows over a flat plate[8] and around a blunt body.[19] The dusty-gas flow in a near-wall jet was studied by Duck *et al.*[20] However, all the numerical results for the cross-flow profile of particle number concentration in dilute suspension flows over a flat wall still contain a nonintegrable singularity on the wall. Foster *et al.*[18] suggested that including the classical Saffman force may not remove the singularity, and a weakly nondilute model is required in order to resolve the singular behavior of particle concentration.

Another important phenomenon peculiar to the motion of a dilute suspension of small noninteracting particles is a possible intersection of particle trajectories and a formation of folds in the pressureless particulate continuum.[21,22] In the cases when the particle trajectories intersect, there form regions, where two different Lagrangian points of the particulate medium are present at the same Eulerian point of space. In the motion of a pressureless medium of noninteracting particles, the trajectories intersect due to the particle inertia. Examples of flows with intersecting particle trajectories can be found in, but not limited to, the cases when there is a strongly nonuniform lift force exerted on a particle, or converging flow of the suspending fluid, or a reflection of particles from a solid surface, or an impact of two particle-laden jets. Experimental evidence of particle trajectory intersections in dilute suspension flows has been revealed in a variety of different fluid-dynamical configurations. For example, in the problem of aerodynamic focusing of small particles in a carrier gas flow through a narrow confining channel particle trajectories cross at a certain common focal point on the symmetry axis of the channel;[23] see also the pioneering experimental work on aerodynamic focusing by Israel and Friedlander.[24] The aerodynamic focusing concept is based on particle inertia and the Stokes drag from the carrier phase.[24] Recently, this concept was extended and the Saffman lift force on lagging particles in a convergent flow was shown to cause the cross-flow particle migration, which enhances focusing.[23] Crossing trajectories have also been observed in the experiments on a grid-generated turbulence in dilute suspensions.[25,26] In the case of a particle-laden flow through a channel, particle trajectories intersect due to particle reflection from the channel walls, which has been observed in experiments.[27] Numerical simulations of dusty-gas flows through confining nozzles[28] and around blunt bodies[29,30] also reveal the origin of crossing particle trajectories due to the particle reflection from rigid surfaces. For both experimental and numerical evidences of crossing particle trajectories, see also the review on erosion of rigid surfaces by particle impact.[31] In the cases described above, a multilayer structure forms in the particulate medium, where two or more initially different parts of the particulate continuum are superimposed, resulting in a fold.

The modified Lagrangian approach was proposed[29] for calculating particle concentration field in the presence of intersecting trajectories. The method is based on integrating particle motion equations along particle trajectories and finding the concentration field from the continuity equation in Lagrangian form. The parts (or layers) of the fold can only be distinguished in Lagrangian variables, because the crossing trajectories have different Lagrangian coordinates but the same Eulerian coordinates at the point of intersection. In addition, the boundary of the region with intersecting trajectories (the boundary of the fold) can easily be found from the condition that the Jacobian of the Eulerian–Lagrangian transformation is zero, i.e., the Jacobian changes sign on the boundary of the fold. The work by Slater and Young[30] discussed advantages and drawbacks of Eulerian methods in comparison with Lagrangian methods to calculate particle concentration fields. The comparison was conducted on an example of a dusty-gas flow around a cylinder in the presence of intersecting trajectories due to the particle rebound from the cylinder surface. It was suggested that the Lagrangian methods are preferable in the case of crossing particle trajectories, because the problem for an Eulerian method is ill posed in the region of trajectory intersections. The work

by Healy and Young[32] presented a comparison of the full Lagrangian method proposed by Osiptsov[29] with another Lagrangian method for calculating particle concentration fields. The study discussed the issue with calculating particle concentration in the presence of crossing particle path lines. Several examples were considered, including particle motion in an inviscid dusty-gas stagnation-point flow and also an inviscid gas-particle flow over a cylinder. The work concluded[32] that the full Lagrangian method[29] is preferable, as it can handle several types of concentration singularity and has a significant potential for dramatic reductions in computational time and improvements in accuracy compared to traditional approach.

The objective of the present work is to construct an asymptotic model of the inertial migration of rigid noncolloidal particles in a dilute suspension flow through the entry region of a channel. We use the two-fluid approach to modeling of suspension flows, where each phase, particles and fluid, is treated as a continuum. The proper expression for the lift force exerted on a particle in a bounded shear flow is an essentially important component of the present study. It will be shown that including the correction to the lift due to the wall effect and a nonzero slip parameter makes it possible to resolve the nonintegrable singularity in the concentration profile *within* the dilute suspension model. In order to calculate the particle concentration and velocity fields, the full Lagrangian approach[29] is used, which can be applied even in the cases of intersection of particle trajectories and formation of singularities in the particle concentration field, when any Eulerian method fails to provide a correct solution.[18,29,30]

This paper is organized as follows. Section II presents the formulation of a problem of the dilute suspension flow in the entry region of a channel. In Sec. III, we derive asymptotic equations governing the dilute suspension flow in a boundary layer on the length scale of particle velocity relaxation. In Sec. IV, the equations of the flow on the length scale of overlapping of boundary layers are presented. The matching conditions are derived. In Sec. V, the full Lagrangian approach for calculating particle concentration fields is described. Section VI presents the numerical results for particle trajectories and the cross-flow particle concentration profile in comparison with existing experimental data and theoretical results. A summary of the results and concluding remarks are given in Sec. VII.

II. FORMULATION OF THE PROBLEM

We consider a two-dimensional steady flow of a dilute suspension of noncolloidal rigid particles in the entry region of a plane channel or a circular pipe. The carrier phase is an incompressible Newtonian fluid. The particles are rigid spheres of constant radius. The ratio of the particle substance density to the fluid density is of the order of unity or significantly larger unity. The velocity relaxation length of a Stokes particle is of the order of the channel width. The volume concentration of particles is small, so the chaotic motion of particles and interactions between particles are neglected. Channel walls are rigid, impermeable, and smooth. The channel Reynolds number based on the mean flow velocity and the channel half-width is assumed to be high, but subcritical, so the flow is assumed to be laminar. Gravity is neglected, because we consider an entry region of a vertical pipe or a horizontal section of a vertical plane channel. At the inlet section of the channel, the profiles of fluid and particle velocity and the particle number concentration are uniform and the particle slip velocity is zero. The flow is considered in the channel entry region, where the boundary layers develop on the channel walls and the Poiseuille velocity profile of the carrier fluid is being established. The goal of this work is to construct an asymptotic model of the inertial migration of particles and to study the evolution of the cross-flow particle concentration profile in the entry region of a channel. In what follows, we will describe the details of the problem formulation and present the equations of the model.

The suspension flow is considered within the two-fluid approach based on the concept of two interpenetrating and interacting continua.[33] Within this approach, a two-phase system is treated as a combination of two continua, where one continuum is related to the carrier fluid and another to suspended particles. As a basis for mathematical modeling of the suspension flow, we will use the asymptotic two-fluid model of a dilute suspension,[13] in which the particle volume concentration c is negligibly small: $c \to 0$. The carrier phase is characterized by the substance density ρ, molecular viscosity μ, and the local velocity $\mathbf{v}=(u,v)$. The suspended particles have radius σ and substance density ρ_s^0. To describe the motion of particles, we introduce the particulate continuum with local velocity $\mathbf{v}_s=(u_s,v_s)$ and local density $\rho_s=mn_s$. Here, m is the mass of a single particle and n_s is the particle number concentration. Hereinafter, the subscript s denotes parameters related to the particulate phase, the superscript 0 denotes parameters related to the particle substance rather than to the particulate medium, and the superscript ∞ denotes dimensional parameters at the channel inlet section. Since the relative volume of the particulate phase is neglected, the local density and viscosity of the carrier fluid are equal to its constant substance density ρ and molecular viscosity μ. We assume that the ratio of the particle substance density to the fluid density $\xi=\rho_s^0/\rho$ is of order unity or significantly larger unity. Additionally, it is an assumption that the characteristic mass load of particles defined as $\alpha=\rho_s^\infty/\rho=c^\infty\xi$ is negligibly small ($\alpha \to 0$) even in the case of a dusty-gas flow. In what follows, it will be shown that in this case the feedback effect of particles upon the carrier fluid can be neglected, and the suspension flow is governed by the so-called one-way coupling model.[13] We will consider separately two cases when the particle-to-fluid density ratio is of order unity (suspension flows) or significantly large unity (dusty-gas flows). In the case of a dusty-gas flow, although the density ratio ξ is significantly larger unity ($\sim 10^3$),[13] the volume concentration of particles c^∞ is sufficiently small ($<10^{-4}$) (Ref. 16) that justifies the assumption of a small mass load α.

It is assumed that the medium of particles is dilute and the Brownian motion, collisions, and interactions between particles are neglected. These assumptions make it possible to simplify significantly the conservation laws and to formulate the relations for the momentum exchange between the phases on the basis of formulas for the forces exerted on a

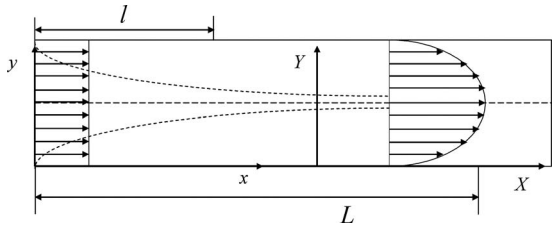

FIG. 1. The sketch of the flow pattern in the channel entry region, where the Poiseuille velocity profile is being established. Arrows: the carrier phase velocity, dashed lines: boundary layers.

single particle. The assumption that the particulate medium is collisionless allows us to neglect internal stresses in the continuum description of the particulate medium.

We introduce the Cartesian coordinate system Oxy fitted to the channel, with the x- and y-axes directed along and normal to the channel walls (Fig. 1). The origin of the coordinate system is located at the inlet on the channel wall.

The equations of the two-fluid model for a dilute suspension flow are written in the dimensional form as follows:[33]

$$\mathrm{div}\ \mathbf{v}=0, \quad \mathrm{div}(\rho_s \mathbf{v}_s)=0,$$
$$\rho(\mathbf{v}\nabla)\mathbf{v}=-\nabla p+\mu\Delta\mathbf{v}-n_s\mathbf{f}_s, \quad m(\mathbf{v}_s\nabla)\mathbf{v}_s=\mathbf{f}_s. \tag{1}$$

Here, $\mathbf{f}_s$ is the total hydrodynamic force exerted on a single particle from the suspending fluid. The term $-n_s\mathbf{f}_s$ on the right-hand side of the Navier–Stokes equation represents the feedback effect of particles upon the carrier fluid. We assume that the momentum exchange between the carrier fluid and particles is due to the drag force, the lift force, the Archimedes force, and the virtual mass force:

$$\mathbf{f}_s=\mathbf{F}_{\mathrm{drag}}+\mathbf{F}_{\mathrm{lift}}+\mathbf{F}_{\mathrm{Arch}}+\mathbf{F}_{\mathrm{vm}},$$

where

$$\mathbf{F}_{\mathrm{drag}}=6\pi\sigma\mu(\mathbf{v}-\mathbf{v}_s)D, \quad \mathbf{F}_{\mathrm{Arch}}=\frac{4}{3}\pi\sigma^3\rho\frac{d\mathbf{v}}{dt},$$
$$\mathbf{F}_{\mathrm{vm}}=\frac{2}{3}\pi\sigma^3\rho\left(\frac{d\mathbf{v}}{dt}-\frac{d\mathbf{v}_s}{dt}\right), \tag{2}$$
$$D=1+\frac{1}{6}\mathrm{Re}_s^{2/3}, \quad \mathrm{Re}_G=\frac{4\rho\sigma^2}{\mu}\frac{\partial u}{\partial y}, \quad \mathrm{Re}_s=\frac{2\sigma|\mathbf{v}-\mathbf{v}_s|\rho}{\mu}.$$

Here, the drag force is given by the widely used Schiller–Nauman formula,[34] also known as the Klyachko formula, which is an empirical extension of the Stokes drag (valid in the range $0<\mathrm{Re}_s<10^3$).[34] In the expression for the virtual mass force, the total derivative is taken along the fluid streamline.[35] Here, we neglect gravity force, assuming that the ratio of the gravity force to the drag force is small compared to unity:

$$\frac{2\rho_s^0\sigma^2 g}{9\mu U}\ll 1.$$

The lift force is written as

$$\mathbf{F}_{\mathrm{lift}}=c_l(\chi,Y_p)\mathbf{F}_{\mathrm{Saff}},$$

$$\mathbf{F}_{\mathrm{Saff}}=6.46\sigma^2\sqrt{\mu\rho}\sqrt{\left|\frac{\partial u}{\partial y}\right|}(u-u_s)\mathrm{sign}\left(\frac{\partial u}{\partial y}\right)\mathbf{j},$$
$$\chi=(u_s-u)\left(\frac{\rho}{\mu}\frac{\partial u}{\partial y}\right)^{-1/2}=\pm\frac{\mathrm{Re}_s}{\mathrm{Re}_G^{1/2}}, \tag{3}$$
$$Y_p=y/L_{\mathrm{Saff}}=y\left(\frac{\rho}{\mu}\frac{\partial u}{\partial y}\right)^{1/2}.$$

Here, $\mathbf{j}$ is the unit vector of the y-axis; χ is positive when the particles lead the fluid and negative otherwise. The correction factor to the lift force accounts for a finite nonzero value of the slip parameter and the wall effect. It will be shown below that the migration of particles essentially takes place in the near-wall regions, where the effect of the curvature of the fluid velocity profile can be neglected.[12] Hence, we can use the results for the lift in a linear shear flow bounded by a single wall.[5–7]

It will be shown below that in the present problem formulation the particles lead the fluid, so $\chi\geq 0$. To fit the numerical data for wall-bounded flows in the case $\chi\geq 0$, we propose the following expression:

$$c_l=c_l^\infty(\chi)(1-n(\chi)\exp[-m(\chi)Y_p]),$$
$$n=1+\frac{1.77\chi}{c_l^\infty}, \quad m=0.453+0.139\chi^{1.93}.$$

The approximation of the numerical results for an unbounded flow is given by[8]

$$c_l^\infty=(1+0.581\chi^2-0.439|\chi|^3+0.203\chi^4)^{-1}.$$

The formula for c_l^∞ agrees well with the numerical data.[5,6] This formula is also in a good agreement with the fit proposed by Mei,[9] and a comparison is illustrated in Fig. 1 of the paper by Asmolov.[19] When $Y_p\to\infty$ (the particle distance from the wall is significantly larger than the Saffman length L_{Saff}), the correction factor c_l is positive and tends to c_l^∞. In the limit $Y_p\to 0$ (the distance to the wall is small compared to L_{Saff} but still large compared to the particle radius σ), the lift coefficient c_l is negative and tends to the value $c_l^0=-1.77\chi$ predicted by Cox and Hsu.[4] Thus, the lift force changes sign on a certain line distanced from the wall, so that particles are repelled from the wall at short distances and pushed toward it at large. Since the lift force is proportional to the particle slip velocity, the particles migrate across streamlines as long as there is a nonzero interphase slip. Hence, the particles may not fully accumulate on the equilibrium line (where the lift force is zero) before the interphase slip vanishes due to the drag force and the phase velocity relaxation is complete.

At the inlet section of the channel ($x=0$), we assume the following conditions: the velocities of fluid and particles are equal, the velocity profile of the fluid (and, hence, of the particles) is uniform, and the particle number concentration is constant across the channel. On the channel walls, the no-slip condition is specified for the carrier phase. Thus, the boundary conditions can be written in the form

$$x=0:\ u=u_s=U,\quad v=v_s=0,\quad \rho_s=\rho_s^{\infty},$$
$$y=0,2d:\ u=v=0. \tag{4}$$

Here, U is the velocity of the fluid and the particulate medium at the inlet section, and d is the channel half-width. Equations for the particulate phase are hyperbolic with the characteristics being particle trajectories. Hence, these equations do not require boundary conditions on the surfaces other than the channel inlet, where the particle trajectories start.

In what follows, we assume that the channel Reynolds number based on the parameters of the carrier flow and the channel half-width is significantly larger unity:

$$\mathrm{Re}=\frac{\rho U d}{\mu},\quad \varepsilon=\frac{1}{\mathrm{Re}}\ll 1.$$

Since the fluid velocity profile at the inlet is uniform and the channel Reynolds number is high, the boundary layers are formed on the channel walls. The present problem formulation is a generalization of the problem of a dusty-gas flow through a channel,[17] which accounts for the following additional complications. The effects of the order-unity density ratio are governed by the Archimedes and the virtual mass forces, which were neglected in the case when the particle-to-fluid density ratio is significantly larger unity (dusty-gas flow[17]). The effects of a boundary on the particle migration are accounted for via the correction factor to the lift force (to resolve the nonintegrable singularity in the cross-flow profile of particle number concentration, which appeared in the earlier models of the two-phase boundary layer[15–18]).

We consider the flow on two different length scales (Fig. 1): (i) the characteristic velocity relaxation length of a Stokes particle $l=mU/6\pi\sigma\mu$, and (ii) the characteristic length of overlapping of the boundary layers $L=d^2U\rho/\mu$.[36] The phase velocity relaxation length scale l defines the region, where a thin boundary layer is formed on the channel wall. Inside the boundary layer, the fluid velocity decreases abruptly due to the no-slip condition on the wall. The particles which initially had a zero slip velocity move faster than the fluid (due to the particle inertia), until the interphase slip vanishes due to the drag force and the velocity relaxation is complete. In the core of the flow, the fluid velocity profile and the particle concentration profile are uniform and the particle slip velocity is zero. The length scale L is the characteristic length, on which the boundary-layer thickness attains the channel half-width, the boundary layers on the upper and lower walls merge (see Fig. 1), and the carrier phase velocity profile develops into that given by the Poiseuille law. We assume that the ratio of the channel half-width d to the velocity relaxation length scale of a Stokes particle l is of order unity: $\lambda=d/l\sim 1$. Then the characteristic length of overlapping of the boundary layers L is significantly larger than the particle velocity relaxation length scale l, since $L/l=\lambda/\varepsilon\gg 1$, as $\varepsilon\to 0$.

Using the method of matched asymptotic expansions,[37] we will construct an asymptotic solution to the problem in the limit $\varepsilon\to 0$.

III. EQUATIONS OF THE FLUID-PARTICLE BOUNDARY LAYER

In this section, we will write, in dimensionless form, the system of equations governing the suspension flow over the velocity relaxation length scale l (Fig. 1), which for spherical particles can be rewritten as

$$l=\frac{2\rho_s^0 U\sigma^2}{9\mu}.$$

The dimensionless variables are introduced by the formulas

$$x'=lx,\quad y'=ly,\quad u'=Uu,\quad v'=Uv,\quad p'=\rho U^2 p,$$
$$u_s'=Uu_s,\quad v_s'=Uv_s,\quad \rho_s'=\rho_s^{\infty}\rho_s,\quad n_s'=n_s^{\infty}n_s. \tag{5}$$

The dimensional variables are denoted by a prime, when it is needed to distinguish them from the dimensionless variables. The flow in a channel is symmetrical with respect to the centerline; hence we will consider only the domain between the centerline and a channel wall. Because the velocity profile of the carrier fluid is convex with a single local maximum on the channel centerline, in the region considered the shear rate is positive: $\partial u/\partial y>0$. In addition, in dimensionless variables it can easily be shown that the particle number concentration is equal to the density of the particulate medium: $n_s=\rho_s$.[17] Thus, in what follows by ρ_s we will also understand the nondimensional particle number concentration. Substituting Eq. (5) into Eqs. (1)–(4), we obtain the following system of dimensionless equations:

$$\mathrm{div}\,\mathbf{v}=0,\quad \mathrm{div}(\rho_s\mathbf{v}_s)=0,\quad (\mathbf{v}\nabla)\mathbf{v}=-\nabla p+\varepsilon\lambda\Delta\mathbf{v}-\alpha\rho_s\mathbf{f}_s,$$
$$(\mathbf{v}_s\nabla)\mathbf{v}_s=\frac{2\xi}{2\xi+1}\left[D(\mathbf{v}-\mathbf{v}_s)+\kappa c_l\sqrt{\frac{\partial u}{\partial y}}(u-u_s)\mathbf{j}\right]+\frac{3}{2\xi+1}(\mathbf{v}\nabla)\mathbf{v}, \tag{6}$$
$$\varepsilon=\frac{\mu}{\rho U d},\quad \lambda=\frac{d}{l},\quad \kappa=\frac{6.46}{2\sqrt{2\pi}}\sqrt{\frac{\rho}{\rho_s^0}}.$$

In the dimensionless form, boundary conditions (4) are rewritten as

$$x=0:\ u=u_s=\rho_s=1,\quad v=v_s=0,\quad y=0,2\lambda:\ u=v=0. \tag{7}$$

Summarizing the assumptions stated in Sec. II, we deal with the following asymptotic limit in terms of the governing dimensionless parameters:

$$\varepsilon=1/\mathrm{Re}\to 0,\quad \lambda=d/l\sim 1,\quad \xi=\rho_s^0/\rho\sim 1,\quad c\to 0,$$
$$\mathrm{Re}_s\to 0,\quad \mathrm{Re}_G\to 0,\quad \chi=\mathrm{Re}_s/\sqrt{\mathrm{Re}_G}\sim 1.$$

The other dimensionless groups entering into the problem formulation can be expressed in terms of these parameters. Taking into account that $\alpha\to 0$, we neglect the feedback term on the right-hand side of the Navier–Stokes equation for the carrier fluid (6). The procedure used to find an asymptotic solution of Eqs. (6) and (7) in the limit $\varepsilon\to 0$ is similar to

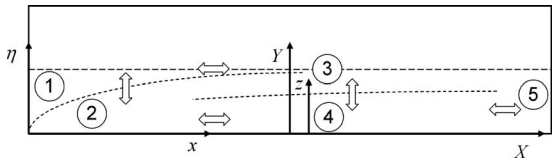

FIG. 2. Different asymptotic domains: (1) entry region, (2) boundary layer, (3) region of overlapping of boundary layers, (4) lower sublayer, and (5) far-downstream region. Symbol ⇔ denotes asymptotic matching of solutions in adjacent domains.

that for the problem of a boundary layer on a flat plate. We separate the flow domain into two regions: the outer region (the core of the flow) and the inner region (the thin boundary layer developing along the channel wall). The outer solution is the uniform free stream: $u=u_s=\rho_s=1$, $v=v_s=0$, and $p=\text{const}$. We seek the inner solution in the form of asymptotic series in the powers of $\varepsilon\lambda$, retaining only the leading terms:

$$y=(\varepsilon\lambda)^{1/2}\eta, \quad u=u_2(x,\eta), \quad v=(\varepsilon\lambda)^{1/2}v_2(x,\eta),$$

$$p=p_2(x,\eta), \quad u_s=u_{s2}(x,\eta), \tag{8}$$

$$v_s=(\varepsilon\lambda)^{1/2}v_{s2}(x,\eta), \quad \rho_s=\rho_{s2}(x,\eta).$$

Hereinafter, the subscripts of the variables indicate the numbers of corresponding asymptotic domains shown in Fig. 2.

Substituting these formulas into Eq. (6) and retaining only the leading terms, we obtain (the subscript 2 is omitted for simplicity):

$$\frac{\partial y}{\partial x}+\frac{\partial v}{\partial \eta}=0, \quad \frac{\partial \rho_s u_s}{\partial x}+\frac{\partial \rho_s v_s}{\partial \eta}=0, \quad u\frac{\partial u}{\partial x}+v\frac{\partial u}{\partial \eta}=\frac{\partial^2 u}{\partial \eta^2},$$

$$\frac{\partial p}{\partial \eta}=0, \quad u_s\frac{\partial u_s}{\partial x}+v_s\frac{\partial u_s}{\partial \eta}=F_{sx},$$

$$F_{sx}=\frac{2\xi}{2\xi+1}D_0(u-u_s)+\frac{3}{2\xi+1}\left(u\frac{\partial u}{\partial x}+v\frac{\partial u}{\partial \eta}\right),$$

$$u_s\frac{\partial v_s}{\partial x}+v_s\frac{\partial v_s}{\partial \eta}=F_{s\eta}, \tag{9}$$

$$F_{s\eta}=\frac{2\xi}{2\xi+1}\left[D_0(v-v_s)+\kappa_0 c_l\sqrt{\frac{\partial u}{\partial \eta}}(u-u_s)\right]+\frac{3}{2\xi+1}\left(u\frac{\partial v}{\partial x}+v\frac{\partial v}{\partial \eta}\right),$$

$$c_l(\chi,x,\eta)=c_l^{\infty}\left(1-n\exp\left[-m_1(\chi)\frac{\eta}{x^{1/4}}\right]\right),$$

$$m_1=m\frac{\sqrt{\varphi''(0)}}{(\varepsilon\lambda)^{1/4}}, \quad \chi=\frac{|u-u_s|}{(\varepsilon\lambda)^{1/4}}, \quad \kappa_0=\frac{6.46}{12\sqrt[4]{18\pi}}\mathrm{Re}_{s0}^{3/2}\left(\frac{\rho_s^0}{\rho}\right)^{1/4},$$

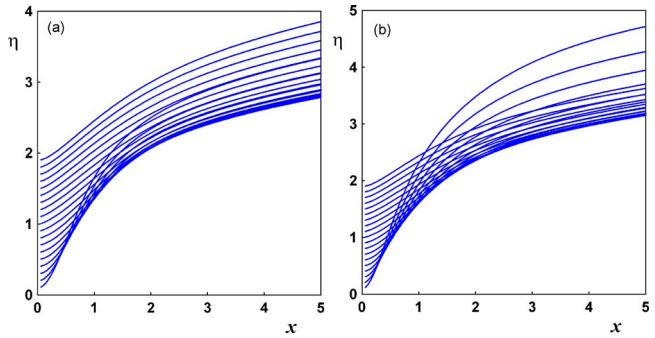

FIG. 3. (Color online) Particle trajectories in the boundary layer for corrected lift force, $\xi\to\infty$, $\kappa_0=5$ (a) and 10 (b)

$$D_0=1+\frac{1}{6}\mathrm{Re}_{s0}^{2/3}(u-u_s)^{2/3}, \quad \mathrm{Re}_{s0}=\frac{2\sigma U\rho}{\mu}.$$

Here, the last terms on the right-hand sides of the momentum equations for the particulate phase correspond to the virtual mass and Archimedes forces. In the strong shear limit ($\chi\ll 1$) and at a significantly large particle-to-fluid density ratio ($\xi\gg 1$), the terms with the virtual mass and Archimedes forces are negligible, the correction factor to the lift force tends to unity ($c_l\to 1$), and the equations of the particulate phase tend to those for a dusty-gas flow.[17] In addition, $\varphi''(0)$ stands for the derivative of the Blasius function.[36] An additional simplification comes from the fact that the outer flow is uniform, so the pressure gradient is zero in the boundary layer. Boundary conditions (7) take the form

$$x=0: \ u_s=\rho_s=1, \quad v_s=0,$$

$$\eta=0: \ \varphi u=v=0, \quad \eta\to\infty: \ u\to 1. \tag{10}$$

IV. EQUATIONS ON THE LENGTH SCALE OF OVERLAPPING OF THE BOUNDARY LAYERS

In this section, we will consider the flow on the characteristic length scale of overlapping of the boundary layers $L=d^2U\rho/\mu$ (Fig. 1). Nondimensional variables are introduced as follows:

$$x'=LX, \quad y=dY', \quad u'=Uu_3, \quad v'=(d/L)Uv_3,$$

$$p'=\rho U^2 p_3, \quad u_s'=Uu_{s3}, \quad v_s'=(d/L)Uv_{s3}, \tag{11}$$

$$\rho_s'=\rho_s^{\infty}\rho_{s3}, \quad n_s'=n_s^{\infty}n_s.$$

The dimensionless variables describing the flow in this region are denoted by the subscript 3 (see Fig. 3). Substituting these formulas into Eqs. (1)–(4) and retaining only the leading terms, we obtain the following equations:

$$\frac{\partial u_3}{\partial X}+\frac{\partial v_3}{\partial Y}=0, \quad u_{s3}\frac{\partial \rho_{s3}}{\partial X}+v_{s3}\frac{\partial \rho_{s3}}{\partial Y}=0,$$

$$u_3\frac{\partial u_3}{\partial X}+v_3\frac{\partial u_3}{\partial Y}=-\frac{dp_3}{dX}+\frac{\partial^2 u_3}{\partial Y^2}, \quad \frac{dp_3}{dY}=0,$$

$$u_3-u_{s3}=0, \quad v_3-v_{s3}=0, \tag{12}$$

$$X=0:\ u_3=1,\quad v_3=0,\quad \rho_{s3}=1;\quad Y=0,\quad 2:\ u_3=v_3=0.$$

From Eq. (12), we find that the phase velocities are equal to within the leading order in this region, and hence the phase velocity relaxation is complete. The boundary conditions at the channel inlet section are derived from the condition of asymptotic matching with the uniform stream at fixed Y and $X\to 0$. The continuity equation for the dispersed phase can be rewritten in the form of the material derivative of the particle number concentration along the fluid streamlines:

$$\frac{d\rho_{s3}}{dt}=0,\quad \frac{dX}{dt}=u_3,\quad \frac{dY}{dt}=v_3.$$

From this equation with boundary conditions (12), we find that the particle number concentration is constant along the fluid streamlines: $\rho_{s3}=1$. Equations of the fluid motion (12) coincide with the formulation of the problem of a viscous incompressible flow in the entry region of a plane channel. An approximate solution to this problem is known.[36] The constant cross-flow particle concentration $\rho_{s3}=1$ is not a uniformly valid asymptotics of the solution of Eq. (12), since near the channel wall a thin sublayer forms, where the particle number concentration deviates from unity due to the inertial migration of particles, which takes place upstream in the boundary layer. This lower sublayer is asymptotically thinner than the channel half-width.

In general, the entire flow domain in the entry region of a channel can be split into five asymptotic domains (Fig. 2): (1) the region of a uniform free stream, where the parameters are the same as in the inlet section (the fluid velocity and particle concentration profiles are uniform and the particle slip velocity is zero), (2) the boundary layer on the channel wall, where the fluid velocity profile is nonuniform, particles lead the fluid, the particle slip velocity is finite compared to the fluid velocity, and hence the migration due to the lift force results in a nonuniform particle concentration profile, (3) the region of overlapping of the boundary layers, where the flow velocity profile attains that given by the Poiseuille law, the particle slip velocity is negligible, and the particle concentration profile is uniform, (4) the lower sublayer, where the fluid velocity profile is linear, the particle slip velocity is negligible, and the particle concentration is nonuniform, and finally, (5) the far-downstream region ($X\gg 1$), where the parameters of fluid and particles are independent of the longitudinal coordinate X, the fluid velocity is given by the Poiseuille law, and the particle concentration is nonuniform over the entire channel half-width.

Next, we derive equations governing the suspension flow in the lower sublayer (region 4, Fig. 2). The new stretched variables are introduced as

$$u_3=(\varepsilon/\lambda)^{1/4}u_4(X,z),\quad v_3=(\varepsilon/\lambda)^{1/2}v_4(X,z),$$

$$Y=(\varepsilon/\lambda)^{1/4}z,\quad u_{s3}=(\varepsilon/\lambda)^{1/4}u_{s4}(X,z),\qquad (13)$$

$$v_{s3}=(\varepsilon/\lambda)^{1/2}v_{s4}(X,z),\quad \rho_{s3}=\rho_{s4}(X,z).$$

The exponents of the leading terms are chosen in accordance with the conditions of asymptotic matching with the solutions in adjacent asymptotic regions. Below, it will be shown explicitly that the particle trajectories in the lower sublayer behave like $X^{1/4}$, which is in accord with the exponents of the leading terms in the above asymptotic expansions. Here and in what follows, we denote the variables corresponding to the flow in the lower sublayer by the subscript 4 (Fig. 2). Substituting expansions (13) into (12) and retaining only the leading terms, we obtain

$$\frac{\partial u_4}{\partial X}+\frac{\partial v_4}{\partial z}=0,\quad \frac{\partial^2 u_4}{\partial z^2}=0,\quad \frac{\partial p_4}{\partial z}=0,$$

$$u_4\frac{\partial \rho_{s4}}{\partial X}+v_4\frac{\partial \rho_{s4}}{\partial z}=0,\quad u_4=u_{s4},\quad v_4=v_{s4},\qquad (14)$$

$$z=0:\ u_4=v_4=0,\quad z\to\infty:\ u_4=u_3|_{Y=0}.$$

The solution of Eq. (14) is $u_4=G(X)z$, $v_4=G'(X)z^2/2$, and ρ_{s4} is constant along the streamlines of the carrier phase. Thus, the fluid velocity profile is linear, the particle slip velocity is negligible, hence the lift force is zero according to formula (3), and the value of the particle number concentration, which enters into the lower sublayer, is then transferred without changing along the fluid streamlines. The concentration profile is stretched in this region, because the fluid streamlines diverge. The condition of asymptotic matching of the velocity in the lower sublayer (region 4, Fig. 2) u_4 with the velocity in the region of overlapping of boundary layers (region 3, Fig. 2) u_3 is written in the form

$$\left.\frac{\partial u_4}{\partial z}\right|_{z\to\infty}=\left.\frac{\partial u_3}{\partial Y}\right|_{Y=0}.$$

From this formula, we find the function $G(X)$

$$G(X)=\left.\frac{\partial u_3}{\partial Y}\right|_{Y=0}.$$

In the lower sublayer, the constant value of ρ_{s4} is transferred along the streamlines of the carrier phase, which are given by the equation for the stream function $\omega=z\sqrt{G(X)}=\text{const}$. This means that the particle number concentration ρ_{s4}, being constant along the streamlines, can be considered as dependent on the stream function ω only, i.e., $\rho_{s4}=\rho_{s4}(\omega)$. The function $\rho_{s4}(\omega)$ should be determined from the condition of asymptotic matching with the solution of the boundary-layer problem (9) and (10) expressed in terms of the stream function. Since the particle number concentration is shown to be nonuniform in a thin near-wall layer, where the velocity profile is linear, then upstream, in the boundary layer, the migration also occurs in a thin near-wall layer, where the velocity profile is linear. This is why we stated above that no correction to the lift force is needed to account for the quadratic profile of the carrier flow. In addition, as the inner longitudinal coordinate x tends to infinity inside the boundary layer, the particle velocity relaxation completes and hence the lift force vanishes according to Eq. (3), so the particles no longer migrate across fluid streamlines. Thus, the particles become frozen into the fluid, and the particle concentration depends on the stream function only.

We will now describe asymptotic matching of solutions for the particle concentration profile between regions 2 and 5

through region 4 (Fig. 2). After matching the solutions in adjacent asymptotic regions and excluding region 4, we will derive the matching condition for the solutions in regions 2 and 5.

In order to match the solutions for the particle concentration in regions 2 and 4, we should find the asymptotics of the solution in region 4 as $X \to 0$ and in region 2 as $x \to \infty$. Then, the condition of matching is the equality of these asymptotics.[37] The asymptotics of the function $G(X)$ as $X \to 0$ is given by[36]

$$G(X) = \frac{\varphi''(0)}{\sqrt{X}}.$$

Taking into account this formula, we write the equation for a streamline $\omega = z\sqrt{G(X)} = \text{const}$ in the limit $X \to 0$ as

$$\omega = \frac{z\sqrt{\varphi''(0)}}{X^{1/4}} = \text{const}, \quad X \to 0. \tag{15}$$

Since it is shown above that $\omega \sim \sqrt{G(X)}$ and $G(X) \sim 1/\sqrt{X}$, there appears the exponent of $\frac{1}{4}$ in Eq. (15). We will now rewrite the expression for the stream function in terms of the inner variables η and x specified inside region 2 (Fig. 2). From the formulas for the length scales chosen to normalize the variables in the boundary layer (8) and in the lower sublayer (11) and (13), we find

$$\theta = \frac{\eta}{x^{1/4}} = \frac{z}{X^{1/4}}.$$

Here, θ is the notation for the stream function in the inner variables of region 2 (Fig. 2). Equation (15) implies that it is convenient to match the solutions for the particle concentration in the variables (x, θ) and (X, ω), for the fixed magnitudes of stream functions θ (region 2, Fig. 2) and ω (region 4, Fig. 2) as $X \to \infty$ and $X \to 0$, respectively. In this asymptotic matching, X is the outer coordinate tending to zero, and x is the inner coordinate tending to infinity, since there is a relation between these coordinates obtained from the expressions for the length scales: $X = \varepsilon x/\lambda$. Hence, we can represent the condition of asymptotic matching of the solutions for the particle concentration in regions 2 and 4 in the form

$$\rho_{s4}(\omega)\big|_{X\to 0} = \rho_{s2}(x,\theta)\big|_{x\to\infty}, \quad \omega = \theta\sqrt{\varphi''(0)}. \tag{16}$$

We introduce the notation

$$\rho_{s2}^{\lim}(\theta) = \lim_{x\to\infty} \rho_{s2}(x,\theta)$$

for the asymptotic profile of the particle concentration, which should be determined from the solution of Eqs. (9) and (10) in the variables (x, θ). Matching condition (16) gives the value of the particle concentration at the entry to the lower sublayer.

Then, according to the solution of Eq. (14), the value of particle concentration is transferred without changing along the streamlines of the carrier fluid throughout region 4 (Fig. 2). In other words, in the entire region 4 the particle concentration depends on the stream function ω only. This makes it possible to track the particle concentration through region 4 (Fig. 2) and to determine the particle concentration distribution far downstream in region 5 at $X \to \infty$ from the matching condition with region 2 at $X \to 0$ (16). As $X \to \infty$, we have $G(X) = 3$.[36] Hence, the equation of streamlines takes the form $\omega = z\sqrt{3} = \text{const}$, as $X \to \infty$. In the far-downstream region 5 (Fig. 2), the Poiseuille velocity profile is fully established and the fluid streamlines are straight lines parallel to the channel walls ($z = \text{const}$). From this equation and the relation between the transverse coordinates z and Y (13), it follows that the solutions in regions 4 and 5 should be matched asymptotically at the fixed ω and Y:

$$\rho_{s4}(\omega)\big|_{X\to\infty} = \rho_{s5}(Y), \quad Y\sqrt{3}\left(\frac{\lambda}{\varepsilon}\right)^{1/4} = \omega.$$

Finally, eliminating the variables of region 4 (Fig. 2), from Eq. (16) we obtain the matching condition for solutions in the boundary layer (region 2) and in the far-downstream zone (region 5)

$$\rho_{s5}(Y) = \rho_{s2}^{\lim}(\theta), \quad Y = \theta\left(\frac{\varepsilon}{\lambda}\right)^{1/4}\left(\frac{\varphi''(0)}{3}\right)^{1/2}. \tag{17}$$

Thus, using the method of matched asymptotic expansions, we have found the relation between the far-downstream cross-channel concentration profile and the concentration profile in the boundary layer. Excluding the lower sublayer (region 4, Fig. 2), we reduced the problem of determining the cross-channel particle concentration profile $\rho_{s5}(Y)$ in the far-downstream region to finding the large-x asymptotics $\rho_{s2}^{\lim}(\theta)$ of the solution to the fluid-particle boundary-layer Eqs. (9) and (10).

V. THE FULL LAGRANGIAN APPROACH FOR CALCULATING PARTICLE VELOCITY AND CONCENTRATION PROFILES

In this section, we will present the method for solving the equations of the two-phase boundary layer (9) and (10) (region 2, Fig. 2). The problem of finding the carrier flow velocity profile is separated from the problem of determining the particle velocity and concentration (one-way coupling model). The velocity field of the carrier fluid is determined from the well-known solution to the Blasius problem of the boundary layer on a flat plate.[36]

When the velocity field of the carrier fluid is found, we can determine the particle velocity and concentration fields. In order to do so, we will use the full Lagrangian approach,[29] which is based on integrating the particle equations of motion along individual particle trajectories and finding particle concentration from the continuity equation in the Lagrangian form. The discussion of this method and comparison with another method can be found in the paper by Healy and Young.[32] In the full Lagrangian approach, the particle equation of motion is integrated along discrete particle trajectories. The particle velocity field is then obtained by repeated application of this procedure for a large number of trajectories, which altogether cover the flow domain with a detailed Lagrangian mesh. An examination[32] of the full Lagrangian approach[29] suggests that it has a number of advantages as compared to Eulerian methods. In particular, the full La-

grangian method allows finding the solution in the case when particle trajectories intersect and a fold of the Lagrangian volume of particulate medium forms. Under these conditions, any Eulerian method would fail to provide a solution.[18,29,30] In addition, the full Lagrangian method reduces the CPU time by orders of magnitude (thereby allowing the calculation of complex three-dimensional flows) and it can handle both steady and unsteady flows without changing the formulation. Being simple yet nontrivial, the method makes possible the interpretation of complex phenomena of particle motion in fluids based on the solution of ordinary differential equations, once the fluid velocity field is known.

Below, we will present the full Lagrangian method in detail. We introduce the new Lagrangian variables (x_0, η_0, τ), where x_0 and η_0 are the initial values of the particle coordinates and τ is the time of particle motion along the trajectory. In the Lagrangian form, the mass and momentum conservation equations for the flow of particulate medium in the boundary layer (9) and (10) are rewritten as

$$\rho_{s0} = \rho_s |J|, \tag{18}$$

$$\frac{dx}{d\tau} = u_s, \quad \frac{d\eta}{d\tau} = v_s, \quad \frac{du_s}{d\tau} = F_{sx}, \quad \frac{dv_s}{d\tau} = F_{s\eta}. \tag{19}$$

Here, ρ_{s0} is the particulate medium density at $\tau=0$, ρ_s is the density of the particulate medium at the actual time instant τ, and J is the Jacobian of the Eulerian–Lagrangian transformation. By the ordinary derivative with respect to τ, we mean here the partial derivative at fixed x_0, η_0. At the initial time instant $\tau=0$, the particle medium element is rectangular with the area equal to $dx_0 d\eta_0$, whereas at a later time instant τ the medium element has become stretched or strained, with the area equal to $|J| dx_0 d\eta_0$, where[29,32]

$$J = J_{xx} J_{\eta\eta} - J_{x\eta} J_{\eta x},$$

$$J_{xx} = \left(\frac{\partial x}{\partial x_0}\right)_{\tau,\eta_0}, \quad J_{x\eta} = \left(\frac{\partial x}{\partial \eta_0}\right)_{\tau,x_0}, \tag{20}$$

$$J_{\eta x} = \left(\frac{\partial \eta}{\partial x_0}\right)_{\tau,\eta_0}, \quad J_{\eta\eta} = \left(\frac{\partial \eta}{\partial \eta_0}\right)_{\tau,x_0}.$$

In these formulas for the components of the Jacobi matrix, the subscripts denote the variables that are held constant in taking the partial derivative. In cases when the particle trajectories intersect, the Jacobian changes sign, while the area remains constant. This is why the absolute value is required in Eq. (18).

The basic idea of the full Lagrangian method is to determine the particle velocity field from the solution of the system of ordinary differential Eq. (19) along the particle trajectories, assuming that the velocity field of the carrier fluid is determined beforehand. The particle medium density ρ_s is then found *algebraically* from Eq. (18) through determining the components of the Jacobi matrix given by Eq. (20).

The procedure of determining the components of the Jacobi matrix is as follows. The continuity equation for the particulate medium in the Eulerian form (9) implies that the stream function $\psi(t, x, \eta)$ can be introduced as follows:

$$\frac{\partial \psi}{\partial \eta} = \rho_s u_s, \quad \frac{\partial \psi}{\partial x} = -\rho_s v_s. \tag{21}$$

In the Lagrangian variables, the stream function is $\psi = \psi(\tau, \eta_0)$. Since the flow under consideration is steady, the stream function depends on η_0 only, $\psi = \psi(\eta_0)$, and we can write the ordinary derivative of ψ with respect to η_0:

$$\frac{d\psi}{d\eta_0} = \frac{\partial \psi}{\partial x}\left(\frac{\partial x}{\partial \eta_0}\right)_{\tau,x_0} + \frac{\partial \psi}{\partial \eta}\left(\frac{\partial \eta}{\partial \eta_0}\right)_{\tau,x_0} = \rho_{s0} u_{s0}.$$

In view of formulas (18), (20), and (21), we rewrite this equation in the form

$$\rho_s \left| \frac{u_s}{u_{s0}} J_{\eta\eta} - \frac{v_s}{u_{s0}} J_{x\eta} \right| = \rho_{s0}. \tag{22}$$

Comparing Eq. (22) to the continuity equation in the Lagrangian form (18), we find two of the four components of the Jacobi matrix

$$J_{xx} = \frac{u_s}{u_{s0}}, \quad J_{\eta x} = \frac{v_s}{u_{s0}}.$$

For the other two components $J_{x\eta}$ and $J_{\eta\eta}$, from Eq. (19) we derive a system of ordinary differential equations, taking partial derivatives with respect to η_0 of both sides of Eq. (19). For simplicity of the equations derived in the Lagrangian variables, we assume that the slip parameter χ is a given constant in the region where the particle migration occurs. Introduce the new variables:

$$e = \frac{\partial x}{\partial \eta_0}, \quad g = \frac{\partial \eta}{\partial \eta_0}, \quad f = \frac{\partial u_s}{\partial \eta_0}, \quad h = \frac{\partial v_s}{\partial \eta_0}.$$

In this notation, Eq. (19) along with the equations for the auxiliary variables are written as

$$\frac{dx}{d\tau} = u_s, \quad \frac{d\eta}{d\tau} = v_s, \quad \frac{du_s}{d\tau} = F_{sx}, \quad \frac{dv_s}{d\tau} = F_{s\eta},$$

$$\frac{de}{d\tau} = f, \quad \frac{dg}{d\tau} = h,$$

$$\frac{df}{d\tau} = \frac{2\xi}{2\xi+1}\left(1 + \frac{5}{18}\mathrm{Re}_{s0}^{2/3}(u-u_s)^{2/3}\right)F + \frac{3}{2\xi+1}\left[\left(\frac{\partial u}{\partial x}e + \frac{\partial u}{\partial \eta}g\right)\frac{\partial u}{\partial x} + u\left(\frac{\partial^2 u}{\partial x^2}e + \frac{\partial^2 u}{\partial x\,\partial \eta}g\right) + \left(\frac{\partial v}{\partial x}e + \frac{\partial v}{\partial \eta}g\right)\frac{\partial u}{\partial \eta} + v\left(\frac{\partial^2 u}{\partial x\,\partial \eta}e + \frac{\partial^2 u}{\partial \eta^2}g\right)\right], \tag{23}$$

$$\frac{dh}{d\tau} = \frac{2\xi}{2\xi+1}\left[D_0 G + \frac{\mathrm{Re}_{s0}^{2/3}(v-v_s)}{9(u-u_s)^{1/3}} F + \kappa_0 c_l \left(\frac{\partial u}{\partial \eta}\right)^{-1/2} \times \left(\frac{H}{2}(u-u_s) + F\frac{\partial u}{\partial \eta} \right) + \kappa_0 \left(\frac{\partial u}{\partial \eta}\right)^{1/2} (u-u_s) \times \left(\frac{n(\chi) m_1(\chi)}{\sqrt[4]{x}} \exp\left[-m_1(\chi) \frac{\eta}{\sqrt[4]{x}} \right] \right) \left(g - \frac{1}{4x} e \right) \right] + \frac{3}{2\xi+1} \left[\left(\frac{\partial u}{\partial x} e + \frac{\partial u}{\partial \eta} g \right) \frac{\partial v}{\partial x} + u \left(\frac{\partial^2 v}{\partial x^2} e + \frac{\partial^2 v}{\partial x\, \partial \eta} g \right) + \left(\frac{\partial v}{\partial x} e + \frac{\partial v}{\partial \eta} g \right) \frac{\partial v}{\partial \eta} + v \left(\frac{\partial^2 v}{\partial x\, \partial \eta} e + \frac{\partial^2 v}{\partial \eta^2} g \right) \right],$$

$$F = \frac{\partial u}{\partial x} e + \frac{\partial u}{\partial \eta} g - f, \quad G = \frac{\partial v}{\partial x} e + \frac{\partial v}{\partial \eta} g - h,$$

$$H = \frac{\partial^2 u}{\partial x\, \partial \eta} e + \frac{\partial^2 u}{\partial \eta^2} g.$$

Thus, we obtain the closed system of eight ordinary differential Eq. (23) along the particle trajectories for the following variables: the particle coordinates x, η and velocities u_s, v_s, the two components of the Jacobi matrix $\partial x/\partial \eta_0$, $\partial \eta/\partial \eta_0$, and two auxiliary variables $\partial u_s/\partial \eta_0$ and $\partial v_s/\partial \eta_0$. These equations can be integrated numerically, and then the particle number concentration ρ_s can be obtained algebraically along the trajectories from the explicit formula (22).

We now have to specify the initial conditions for the unknown variables. The initial conditions for the coordinates and the velocity components are already prescribed in the formulation of the boundary-layer Eq. (10). Differentiating these equations with respect to η_0, we find the necessary initial conditions for the components of the Jacobi matrix and the auxiliary variables. In the case under consideration, it is simple to derive the initial conditions, since the flow at the inlet is uniform, and it would be a more complicated task otherwise. In terms of the new variables, the initial conditions for all unknown variables are rewritten as

$$\tau = 0: \; x = 0, \quad \eta = \eta_0, \quad u_s = 1, \quad v_s = 0, \qquad e = 0, \quad f = 0, \quad g = 1, \quad h = 0. \tag{24}$$

The Cauchy problem (23) and (24) for ordinary differential equations can be solved, once the carrier-fluid velocity and its gradients are known from the solution of the Blasius problem,[36] which represents the boundary-value problem for a third-order ordinary differential equation. The Blasius problem is solved using a variant of the shooting method. The unknown initial condition for the second derivative of the Blasius function is found to be $\varphi''(0) = 0.332\,057$. The carrier-fluid velocity field and its gradients entering into the right-hand sides of Eq. (23) are expressed in terms of the Blasius function φ and its first and second derivatives, which are found explicitly from the solution of the Blasius problem. Thus, the procedure of determining the gradients of the velocity field does not require numerical differentiation. Equation (23) with initial condition (24) is solved using the fourth order Runge–Kutta method. The particle concentration is found from explicit formula (22). Section VI describes the results obtained numerically from Eqs. (22)–(24).

VI. NUMERICAL RESULTS AND DISCUSSION

In this section, the results obtained using the numerical procedure for solving Eqs. (22)–(24) along the particle trajectories are presented in comparison with existing experimental data and theoretical studies by other authors. In numerical calculations, we assumed that governing dimensional parameters belong to the following ranges: $\sigma = 10^{-4} \div 10^{-3}$ m, $\mu = 10^{\div 3} \div 10^{-1}$ Pa s (for fluid) or $\mu = 1.7 \times 10^{-5}$ Pa s (for gas), $\rho = 10^3$ kg/m^3 (for fluid) or $\rho = 1.2$ kg/m^3 (for gas), $\rho_s^0 = 1 \times 10^3 \div 4 \times 10^3$ kg/m^3, $U = 0.1 \div 10$ m/s. Hence, the dimensionless governing parameters may take the values from the ranges: $\kappa_0 = 0.02 \div 44$ and $\xi = 1 \div 3000$.

A. Numerical results

We first present the numerical results for particle trajectories and the cross-flow profile of particle number concentration obtained for the case when the particle-to-fluid density ratio $\xi = \rho_s^0/\rho$ is significantly larger unity (dusty-gas flow), and then follows a description of the results for the case when ξ is of order unity (suspension flow). In the case of a dusty-gas flow ($\xi \to \infty$), the virtual mass force and the Archimedes force can be neglected in Eq. (23). In the numerical calculations described below, the slip parameter was assumed to be equal to a finite nonzero constant for simplification, so that $m_1 = 0.5$ and $n = 2.7$.

We note that Eq. (23) is written for a general case of small but nonzero Re_{s0} with account for the correction to the Stokes drag (in the Schiller–Nauman form); however, in calculations, we studied the effect of this correction and concluded that there is only a slight quantitative effect, which is in accord with the previous work.[17] For this reason, all further results are presented for the classical Stokes drag with no correction.

Figure 3 shows the particle trajectories obtained numerically for $\kappa_0 = 5$ and 10. The case of $\kappa_0 = 5$ and $\xi \to \infty$ corresponds, for example, to the following set of dimensional parameters: $\sigma = 10^{-4}$ m, $\mu = 1.7 \times 10^{-5}$ Pa s, $\rho = 1.2$ kg/m^3, and $\rho_s^0 = 2.5 \times 10^3$ kg/m^3, $U = 1.9$ m/s. Similarly, for a given set of parameters of the gas and particles the flow velocity U corresponding to other values of κ_0 can be found from the formula (9) for κ_0. Figure 3 reveals the formation of a particle-free layer near the wall, which is confirmed by the numerical results for the cross-flow profile of particle number concentration presented in Fig. 4. Particles, which were originally near the wall, are pushed toward the core of the flow under the action of the lift force. Particle trajectories intersect and a fold in the Lagrangian volume of the particulate medium forms, i.e., at any point of space inside the fold, there are two different Lagrangian points of particulate medium with different number concentration and velocity. In this case, any Eulerian method would not provide an accu-

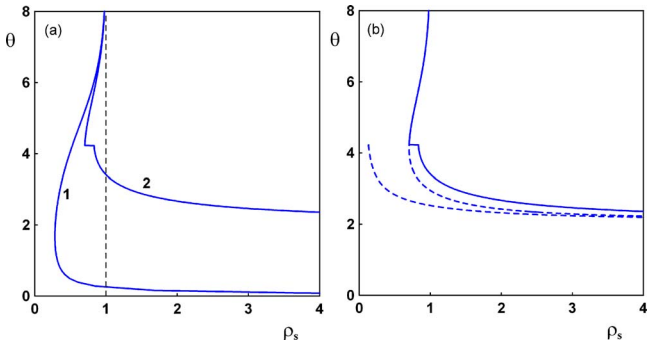

FIG. 4. (Color online) Far-downstream asymptotics of the particle number concentration ρ_s vs the stream function θ in the boundary layer, $\kappa_0=20$, $\xi\to\infty$; (a) lift force is taken in classical Saffman form (curve 1) or with correction factor (curve 2); (b) corrected lift force, concentration profiles in each part of the fold of particulate medium (dashed) and total concentration profile (solid).

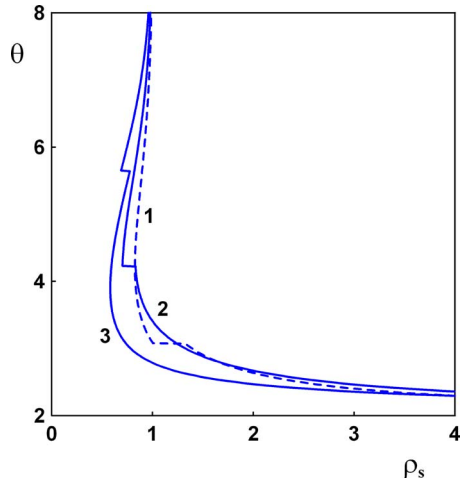

FIG. 5. (Color online) Far-downstream asymptotics of the particle number concentration ρ_s vs the stream function θ in the boundary layer: corrected lift force, $\xi\to\infty$, $\kappa_0=10$, 20, and 40 (curves 1–3).

rate solution, because it requires solving particle medium equations in each part of the fold with a free boundary, which is unknown *a priori*.

In Fig. 4(a), we present the profile of particle number concentration calculated with the classical Saffman force (curve 1), which coincides with that obtained previously in the problem of a dusty-gas flow.[17] In the profile of particle number concentration, there is a nonintegrable singularity[18] on the wall meaning that the model is nonuniformly valid near the channel wall and a correction should be included to account for the presence of the boundary. The number concentration profile for the lift force with the nonzero correction factor c_l (curve 2) shows that migration results in the formation of a particle-free layer near the wall and a fold of the particulate medium above the line, where the lift force changes sign. Figure 4(b) shows the number concentration profiles in each part of the fold and the total concentration profile obtained as a sum of the number concentrations in both parts of the fold. The dashed curve ending abruptly represents the concentration profile in that part of the fold that was originally located near the wall and then was pushed by the lift force into the core of the flow. The asymptote and the jump of the profile of the total number concentration correspond to the lower and the upper boundaries of the fold of particulate medium, respectively. The correction factor c_l, being a function of the transverse coordinate, is positive near the wall and negative far from the wall, changing the sign on a certain line distanced from the wall. The particles migrate toward the line where the lift force is zero, however the particles do not fully accumulate on this line before the particle velocity relaxation is complete and the lift force vanishes.

All the particles, which were originally under the equilibrium line, do not accumulate near this line but are pushed above. This effect is due to the particle inertia. Since the fluid-particle boundary-layer equations are identical both for channel and pipe geometries (with a difference being in the continuity equation only), all the considerations presented above can be applied to an axisymmetric flow in a circular pipe.[17] Thus, the results obtained can be interpreted as follows: the inertial migration of particles in a suspension flow through the entry region of a plane channel or a circular pipe results in the particle accumulation on two symmetric planes (a narrow annulus) distanced from the walls, with a nonuniform concentration distribution between the planes (inside the annulus) and particle-free layers near the walls.

The effect of the coefficient κ_0 with the lift force on the distribution of particle number concentration is shown in Fig. 5. The plot shows that the higher the value of κ_0, the wider the fold of the particulate medium. With an increase in the relative inertia of particles, the depth of penetration of particles into the region above the equilibrium line increases.

In Fig. 6, we present the particle concentration profile for the case of a suspension flow when the particle-to-fluid density ratio is of order unity. Compared to the dusty-gas flow when the particle-to-fluid density ratio is significantly larger unity (Fig. 4), there is an additional nonuniformity, namely, a local maximum appears to be in the concentration

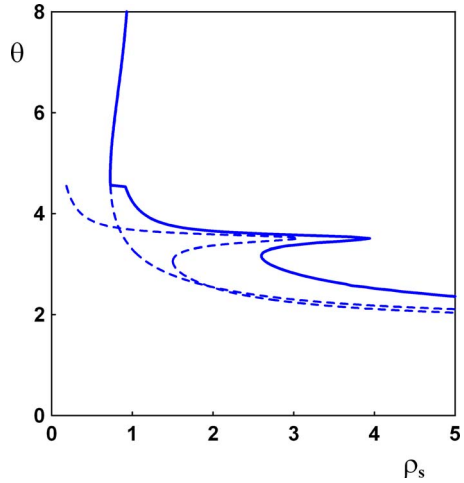

FIG. 6. (Color online) Far-downstream asymptotics of the particle number concentration ρ_s vs the stream function θ in the boundary layer: corrected lift force, $\kappa_0=20$, $\xi=4$. Concentration profiles in each part of the fold of particulate medium (broken curves) and total concentration profile (solid curve).

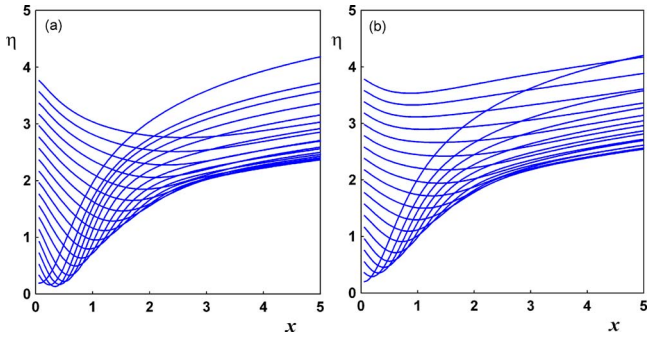

FIG. 7. (Color online) Particle trajectories in the boundary layer for corrected lift force, $\kappa_0=10$, $\xi=3$ (a), and $\xi=5$ (b).

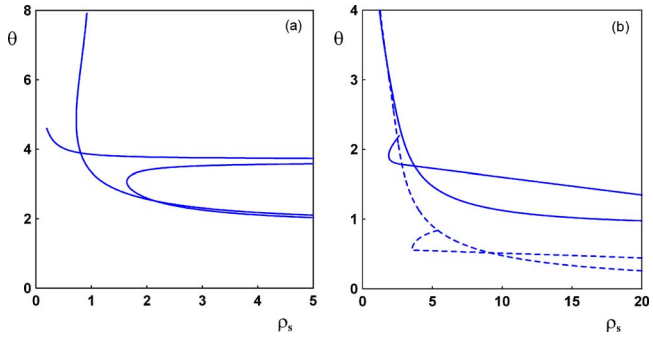

FIG. 9. (Color online) Far-downstream asymptotics of the particle number concentration ρ_s vs the stream function θ in the boundary layer: corrected lift force, concentration profiles in each part of the fold of particulate medium: (a) $\kappa_0=20$, $\xi=3.5$; (b) $\xi=1$, $\kappa_0=1$ (dashed) and $\kappa_0=5$ (solid).

profile. We note that the position of the annulus of particle accumulation, which separates the particle-free layer and the particle-laden fluid, is independent of the particle-to-fluid density ratio. From the plot of particle concentration profiles in each part (layer) of the fold of the particulate medium, it is clear that the nonuniformity arises in that layer of the fold that was initially located below the equilibrium line.

In this case, the particle trajectory pattern shown in Fig. 7 differs noticeably from that for the dusty-gas flow (Fig. 3). The reason is that, when the particle-to-fluid density ratio ξ is of order unity, there is an additional term in the momentum equations for the particulate medium, which is due to the virtual mass force and the Archimedes force [see Eq. (9)]. This term is proportional to the fluid acceleration. In the projection on η, the fluid acceleration is negative in the boundary layer. Hence, this term can be considered as an additional lift force directed toward the wall. The smaller the value of ξ, the larger the coefficient associated with this term, and hence the more pronounced the migration toward the wall in the initial section, which is absent in the case of a dusty-gas flow (see Fig. 3). With increasing ξ, the pattern of particle trajectories tends to that for the case of $\xi\to\infty$ shown in Fig. 3. The effect of the variation of the density ratio on the distribution of particle number concentration is illustrated in Fig. 8. As $\xi\to\infty$, the local maximum in the concentration profile vanishes and the profile tends to that given in Fig. 4. However, for large values of κ_0 with a decrease in the particle-to-fluid density ratio, the local maximum increases [see Fig. 9(a)]. The particle number concentration tends to infinity in a small vicinity of a certain line distanced from the line of particle accumulation, which separates the particle-free near-wall region and the particle-laden fluid.

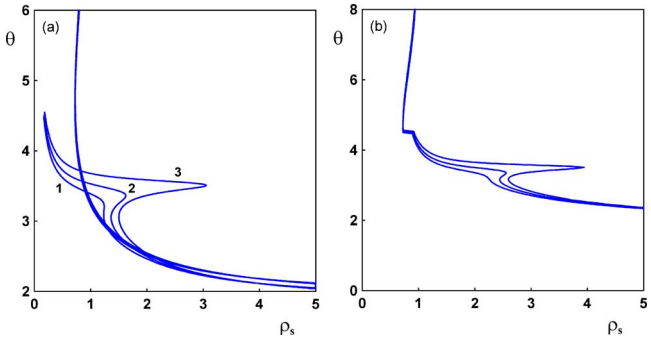

FIG. 8. (Color online) Far-downstream asymptotics of the particle number concentration ρ_s vs the stream function θ in the boundary layer: corrected lift force, $\kappa_0=20$, and $\xi=5$, 4.5, 4 (curves 1–3). Concentration profiles in each part of the fold of particulate medium (a) and total concentration profiles (b).

In Fig. 9(b), we illustrate the concentration profile in the neutrally buoyant case. With an increase in κ_0, an additional local maximum of the number concentration forms inside the fold, and the concentration profile is qualitatively similar to those shown in Figs. 8 and 9(a). The case $\kappa_0=1$ and $\xi=1$ shown in Fig. 9(b) corresponds, for example, to the following set of dimensional parameters: $\sigma=10^{-3}$ m, $\mu=10^{-3}$ Pa s, $\rho_s^0=\rho=10^3$ kg/m^3, and $U=0.02$ m/s. Thus, when the density ratio is of order unity, particles accumulate not only on the two planes (an annulus) as shown in Figs. 4 and 5 but also on two additional planes located closer to the channel centerline (an inner annulus), as shown in Figs. 8 and 9(a).

Next, we demonstrate the relation between the large-x asymptotics of the concentration profile in the boundary layer and the far-downstream cross-channel concentration profile. Equation (17) can be rewritten as follows:

$$\rho_{s5}(Y)=\rho_{s2}^{\lim}(\theta),\quad Y=\theta\left(\frac{\varepsilon}{\lambda}\right)^{1/4}\left(\frac{\varphi''(0)}{q}\right)^{1/2},\tag{25}$$

where $q=3$ for the flow in a plane channel and $q=4$ for the flow through a circular pipe. This equation makes it possible to obtain the cross-channel concentration profile in the far-downstream region for any ε and λ at fixed values of κ_0 and ξ by stretching the cross-flow coordinate.

The quantitative result provided by the present model is the width of the particle-free layer in the far-downstream region 5 (Fig. 2). The thickness of this layer can be calculated from the formula for the Saffman lift force with the correction factor [see Eq. (9)] and the expression (25) relating concentration profiles in the boundary layer 2 and in the far-downstream region 5 (Fig. 2). The asymptote of the concentration profile, which marks the boundary of the particle-free layer, can be found from the condition that the lift force is zero on this line:

$$\theta_{\text{ann}} = \frac{\ln n(\chi)}{m_1(\chi)}.$$

Here, χ is a mean value of the slip parameter. In our simulations, we assumed that the slip parameter is a given constant, so $\theta_{\text{ann}}=2$ for all the results. This assumption makes it possible to obtain an approximate width of the particle-free layer near the wall. Substituting this formula into Eq. (25), we obtain the width of the particle-free layer scaled by the channel half-width (radius):

$$Y_{ann} = \frac{\ln n(\chi)}{m_1(\chi)}\left(\frac{\varepsilon}{\lambda}\right)^{1/4}\left(\frac{\varphi''(0)}{q}\right)^{1/2}. \tag{26}$$

B. Comparison with experiments

We will now compare the numerical results with available experimental data on dilute suspension flows in channels. The work of Matas *et al.*[38] was aimed at studying the migration of neutrally buoyant particles moving in a Poiseuille flow with zero longitudinal slip velocity under the action of the inertial lift force due to the particle rotation in a shear flow (the lift on a neutrally buoyant particle[10–12]). In their experiment, the longitudinal length scale was assumed to be significantly larger than the entry region length to allow the particles to accumulate on the Segre–Silberberg annulus[2] under the action of this lift force. Experiments[38] demonstrated the formation of the particle-free near-wall layer and particle accumulation on an annulus distanced from the pipe wall. There is an analogy between the experimental data[38] and the present theoretical results, because both the lift force on a neutrally buoyant particle and the Saffman lift with a correction factor due to the presence of the wall and a nonzero slip parameter have a similar dependence on the cross-flow coordinate. Both forces are positive near the wall and negative far from the wall, with an equilibrium position being at a certain distance from the wall. A direct comparison does not appear to be possible in this case because the experimental results for the cross-flow concentration field are presented at a distance from the inlet, which is significantly larger than the channel entry length. As a result, the concentration pattern formed at the exit from the entry region is then changed under the action of the lift on a neutrally buoyant particle, but retaining the original qualitative features (annulus, particle-free near-wall layers).

Experiments[38] revealed also the formation of an inner annulus, on which the particles accumulate. It was suggested that the inner annulus is another equilibrium position, which so far is not predicted by the theory. A surprising outcome of our simulations is obtaining an inner annulus that formed due to the action of the virtual mass force and the Archimedes force, as the particle-to-fluid density ratio is decreased to reach the values of order unity. However, at present we are not able either to confirm or to contradict the statement that this inner annulus predicted by the model in the entry region survives under the action of the lift force on a neutrally buoyant particle and gives rise to the concentration pattern in the downstream region registered in the experiments.[38] In our opinion, an experimental work that would focus on measuring the particle distribution *within* the entry region of a channel is required to validate the predictions of the present theory, or to extend our theory to find out what effects give rise to the far-downstream patterns found in previous experiments.[38]

C. Comparison with previous theoretical work

In earlier studies of the two-phase boundary layer, the authors took into account either the Stokes drag only[15] or the Stokes drag and the classical Saffman lift,[17] which resulted in a nonintegrable singularity in the profile of particle number concentration on the wall.[16,18] In the present work, we obtained the cross-flow concentration profile with the particle-free near-wall layer and the singularity of the number concentration at a certain line distanced from the wall, which marks the boundary of the fold of the particulate medium (Figs. 4–6).

We will now derive the asymptotics of the particle number concentration near the singularity line. Consider a thin layer above the singularity line. The normal component of the fluid velocity is a finite constant within this layer, while the normal velocity of particles is small and is exactly zero on the singularity line, because the lift force changes sign on this line. Introduce the new stretched variables in the thin layer: $\eta-\eta_0=\delta\eta_1$, $\nu_s=\sqrt{\delta}\nu_{s1}$. Here, $\delta\to 0$ is an auxiliary small parameter, and ν_{s1} and η_1 are the normal component of the particle velocity and the normal coordinate measured from the singularity η_0, respectively. Substituting these expressions into Eq. (9) and neglecting the higher-order terms, we obtain the reduced asymptotic equations:

$$\nu_{s1}\frac{\partial \nu_{s1}}{\partial \eta_1} \sim \nu, \quad \frac{\partial \rho_s v_{s1}}{\partial \eta_1} \sim 0.$$

The exponents in the expansions of the inner variables in ε are chosen from the condition that the resulting asymptotic equations are consistent and least degenerate.[37] From these equations, we find the local asymptotics near the singularity line:

$$\nu_{s1} \sim \sqrt{\eta_1}, \quad \rho_s \sim 1/\sqrt{\eta_1}, \quad \eta_1 \to 0. \tag{27}$$

Thus, we conclude that the asymptotics of the particle number concentration near the singularity line given by Eq. (27) is *integrable*. Hence, according to the explicit formulas relating the mean distance between particles with the parameters characterizing the concentration singularity,[16] the characteristic distance between particles remains significantly larger than the particle diameter. This statement means that, although the particle number concentration grows unbounded as the fold boundary is approached, the dilute suspension approximation holds true.[16]

Chernyshenko[39] considered the integrability of a particle concentration singularity in a dusty-gas flow near a blunt body in the presence of particle reflection from the body surface. He derived that, in the vicinity of an envelope of particle trajectories, the particle concentration has also an inverse square-root-like behavior, which is governed by Eq. (27). Hence, the above conclusion that the particle concentration singularity on the fold inside the stream is integrable

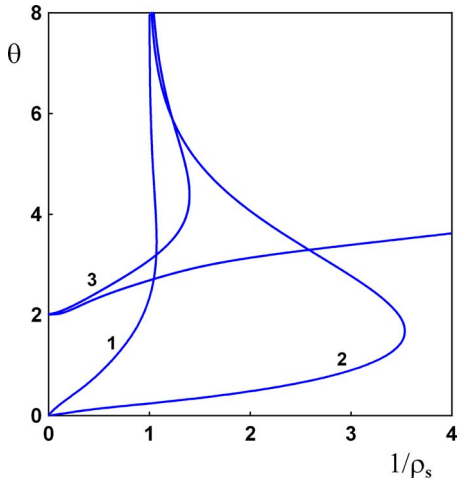

FIG. 10. (Color online) Far-downstream asymptotics of the inversed particle number concentration $1/\rho_s$ vs the stream function θ in the boundary layer. Curves 1–3: Stokes force only, classical Saffman force additionally, and corrected lift force (concentration in each part of the fold), $\kappa_0=20$, $\xi\to\infty$.

appears to be general for any fold of a particulate medium, which is inclined to the flow of the carrier fluid (i.e., on which the normal component of the fluid velocity is nonzero) regardless of the physical phenomenon resulting in the fold, whether it is the lift force pushing the particles from the wall or the reflection of particles from a solid boundary.

The asymptotic behavior (27) is confirmed by the numerical results. In Fig. 10, we plot the inverse particle concentration obtained numerically in the case $\xi=\rho_s^0/\rho\to\infty$ (to allow a comparison with the previous results for dusty-gas flows) with (i) the Stokes drag only,[15] (ii) the Stokes drag and the classical Saffman lift,[17] and (iii) the result of the present work with the corrected lift force. Figure 10 shows the linear behavior of the inverse particle concentration in the vicinity of the singularity $1/\rho_s\sim\eta$ as $\eta\to 0$ in the cases (i) and (ii) (which means that the integral of the concentration $\rho_s\sim 1/\eta$ is divergent at the singularity point $\eta=0$) and the square-root-like behavior predicted by Eq. (27) in the present case (iii).

The result with the integrable distribution of particle number concentration makes a difference to the previous studies of the evolution of a particle concentration profile in the two-phase boundary layer.[15–18] All the existing results for the particle concentration profile contain the nonintegrable singularity on the wall, because either no lift force or a classical Saffman lift was included. In the present work, we demonstrate that the nonintegrable singularity on the wall can be resolved and a self-consistent result for the particle concentration profile can be obtained *within* the dilute suspension approximation by including a proper correction to the lift force due to the presence of a boundary and a nonzero slip parameter.

VII. SUMMARY AND CONCLUSIONS

Within the two-fluid approach, an asymptotic model of the inertial migration of rigid noncolloidal particles in a dilute suspension flow through the channel entry region is constructed. In the momentum exchange between the phases, the drag force, the virtual mass force, the Archimedes force, and the inertial lift force are included, the latter with a correction factor for bounded flows at an arbitrary slip parameter. The solution is constructed using the method of matched asymptotic expansions in the limit of a high channel Reynolds number, the particle-to-fluid density ratio of order unity or significantly larger unity, and the particle velocity relaxation length of the order of the channel width. The problem of finding the cross-channel concentration profile in the far-downstream region, where the Poiseuille velocity profile is fully established, is reduced to solving the equations of the fluid-particle boundary layer developing on the channel wall.

The full Lagrangian approach is used for calculating particle concentration fields. The problem is reduced to a system of ordinary differential equations along particle trajectories for the particle coordinates and velocity components, and the components of the Jacobian of the Eulerian–Lagrangian transformation. The equations are solved numerically. The particle concentration is then calculated algebraically along particle trajectories from the continuity equation in the Lagrangian form. The method makes it possible to calculate particle concentration profiles even in the cases when particle trajectories intersect and folds in the particulate medium form.

The particle trajectory pattern and the evolution of the cross-flow concentration profile are studied for the cases when the particle-to-fluid density ratio is of order unity or significantly larger unity, corresponding to dilute suspension flows and dusty-gas flows, respectively. In the case of a dusty-gas flow, the virtual mass force and the Archimedes force are negligible. In both cases, it is shown that the particle trajectories intersect and a fold in the particulate medium and a particle-free layer near the channel wall form. The cross-flow profile of particle number concentration is found to contain a singularity on the fold boundary at a distance from the wall. It is shown analytically and confirmed numerically that the particle number concentration behaves like an inverse square root of the cross-flow coordinate measured from the singularity. Hence, the particle number concentration is integrable and the dilute suspension approximation holds true. This is in contrast to previous studies of the dusty-gas boundary-layer problem, in which the account of either the Stokes drag only or the classical Saffman lift additionally resulted in a nonintegrable singularity in the particle concentration profile on the wall. We note that the singularity on the wall is resolved within the dilute suspension model essentially due to the effects of the boundary and the nonzero slip parameter accounted for via the correction to the Saffman lift force. In the case when the particle-to-fluid density ratio is of order unity, all four interphase forces are important. It is demonstrated numerically that an additional local maximum appears to be in the particle concentration profile near the singularity line, which is absent in the case when the particle-to-fluid density ratio is significantly larger unity. The concentration at the inner maximum increases as the particle-to-fluid density ratio is decreased. The concentration singularity at the boundary of the particle-laden region remains integrable regardless of the magnitude of the density ratio.

Thus, the inertial migration of particles in a dilute suspension flow through the channel entry region results in particle accumulation on two symmetric planes (an annulus) distanced from the walls, with a nonuniform concentration distribution between the planes (inside the annulus) and particle-free layers near the walls. These numerical results are compared to the tubular pinch effect observed in experiments, and a qualitative analogy is found.

ACKNOWLEDGMENTS

The first author acknowledges M. Thiercelin, E. Borisova, and E. Siebrits for their encouragement to take up an activity on modeling of particle transport. The authors are grateful to J. R. A. Pearson, P. Hammond, and J. Crawshaw for fruitful discussions on the results and many helpful comments. The authors thank Schlumberger for permission to publish.

[1] L. G. Leal, "Particle motions in a viscous fluid," Annu. Rev. Fluid Mech. **12**, 435 (1980).
[2] G. Segre and A. Silberberg, "Behaviour of macroscopic rigid spheres in Poiseuille flow. Pt. 2. Experimental results and interpretation," J. Fluid Mech. **14**, 136 (1962).
[3] P. G. Saffman, "The lift on a small sphere in a slow shear flow," J. Fluid Mech. **22**, 385 (1965); **31**, 624(E) (1968).
[4] R. G. Cox and S. K. Hsu, "The lateral migration of solid particles in a laminar flow near a plane," Int. J. Multiphase Flow **3**, 201 (1977).
[5] E. S. Asmolov, "Dynamics of a spherical particle in a laminar boundary layer," Fluid Dyn. **25**, 886 (1990).
[6] J. B. McLaughlin, "Inertial migration of a small sphere in linear shear flows," J. Fluid Mech. **224**, 261 (1991).
[7] J. B. McLaughlin, "The lift on a small sphere in wall-bounded linear shear flows," J. Fluid Mech. **246**, 249 (1993).
[8] E. S. Asmolov, "Motion of a suspension in the laminar boundary layer on a flat plate," Fluid Dyn. **27**, 49 (1992).
[9] R. Mei, "An approximate expression for the shear lift force on a spherical particle at finite Reynolds number," Int. J. Multiphase Flow **18**, 145 (1992).
[10] J. A. Schonberg and E. J. Hinch, "Inertial migration of a sphere in Poiseuille flow," J. Fluid Mech. **203**, 517 (1989).
[11] A. J. Hogg, "The inertial migration of neutrally-buoyant spherical particles in two-dimensional shear flows," J. Fluid Mech. **272**, 285 (1994).
[12] E. S. Asmolov, "The inertial lift on a spherical particle in a plane Poiseuille flow at large channel Reynolds number," J. Fluid Mech. **381**, 63 (1999).
[13] F. E. Marble, "Dynamics of dusty gases," Annu. Rev. Fluid Mech. **2**, 397 (1970).
[14] A. N. Osiptsov, "Mathematical modeling of dusty-gas boundary layers," Appl. Mech. Rev. **50**, 357 (1997).
[15] A. N. Osiptsov, "Structure of the laminar boundary layer of a disperse medium on a flat plate," Fluid Dyn. **15**, 512 (1980).
[16] A. N. Osiptsov, "Investigation of regions of unbounded growth of the particle concentration in disperse flows," Fluid Dyn. **19**, 378 (1984).
[17] A. N. Osiptsov, "Motion of a dusty gas at the entrance to a flat channel and a circular pipe," Fluid Dyn. **23**, 867 (1988).
[18] M. R. Foster, P. W. Duck, and R. E. Hewitt, "Boundary layers in a dilute particle suspension," Proc. R. Soc. London, Ser. A **462**, 1145 (2006).
[19] E. S. Asmolov, "Dusty gas flow in a laminar boundary layer over a blunt body," J. Fluid Mech. **305**, 29 (1995).
[20] P. W. Duck, R. E. Hewitt, and M. R. Foster, "On the spatial development of a dusty wall jet," J. Fluid Mech. **514**, 385 (2004).
[21] Ya. B. Zel'dovich and A. D. Myshkis, *Elements of Mathematical Physics: A Medium of Non-Interacting Particles* (Nauka, Moscow, 1973) (in Russian).
[22] V. I. Arnold, *Catastrophe Theory* (Springer-Verlag, Berlin, 1992).
[23] I. S. Akhatov, J. M. Hoey, O. F. Swenson, and D. L. Schulz, "Aerosol flow through a long micro-capillary: collimated aerosol beam," Microfluid. Nanofluid. **5**, 215 (2008).
[24] G. W. Israel and S. K. Friedlander, "High-speed beams of small particles," J. Colloid Interface Sci. **24**, 330 (1967).
[25] W. H. Snyder and J. L. Lumley, "Some measurements of particle velocity autocorrelation functions in a turbulent flow," J. Fluid Mech. **48**, 41 (1971).
[26] M. R. Wells and D. E. Stock, "The effects of crossing trajectories on the dispersion of particles in a turbulent flow," J. Fluid Mech. **136**, 31 (1983).
[27] M. Sommerfeld and N. Huber, "Experimental analysis and modeling of particle-wall collisions," Int. J. Multiphase Flow **25**, 1457 (1999).
[28] A. A. Verevkin and Yu. M. Tsirkunov, "Flow of a dispersed phase in the Laval nozzle and in the test section of a two-phase hypersonic shock tunnel," J. Appl. Mech. Tech. Phys. **49**, 789 (2008).
[29] A. N. Osiptsov, "Lagrangian modelling of dust admixture in gas flows," Astrophys. Space Sci. **274**, 377 (2000).
[30] S. A. Slater and J. B. Young, "The calculation of particle transport in dilute gas-particle flows," Int. J. Multiphase Flow **27**, 61 (2001).
[31] J. A. C. Humphrey, "Fundamentals of fluid motion in erosion by solid particle impact," Int. J. Heat Fluid Flow **11**, 170 (1990).
[32] D. P. Healy and J. B. Young, "Full Lagrangian methods for calculating particle concentration fields in dilute gas-particle flows," Proc. R. Soc. London, Ser. A **461**, 2197 (2005).
[33] R. I. Nigmatulin, *Dynamics of Multiphase Continua* (Hemisphere, New York, 1991).
[34] E. E. Michaelides, "Hydrodynamic force and heat/mass transfer from particles, bubbles, and drops—the Freeman scholar lecture," ASME J. Fluids Eng. **125**, 209 (2003).
[35] M. R. Maxey and J. J. Riley, "Equation of motion for a small rigid sphere in a nonuniform flow," Phys. Fluids **26**, 883 (1983).
[36] H. T. Schlichting and K. Gersten, *Boundary-Layer Theory* (Springer-Verlag, Berlin, 2000).
[37] M. Van Dyke, *Perturbation Methods in Fluid Mechanics* (Parabolic, Stanford, CA, 1975).
[38] J.-P. Matas, J. F. Morris, and E. Guazzelli, "Inertial migration of rigid spherical particles in Poiseuille flow," J. Fluid Mech. **515**, 171 (2004).
[39] S. I. Chernyshenko, "Mean distance between particles in dusty gas in the presence of singularities of the distributed particle density," Vestn. Mosk. Univ., Ser. 1: Mat., Mekh. **1**, 69 (1984) (in Russian).